# SUPPORTING INFORMATION

FIGURE S1. Mean (red; mean of all experiments) and individual (gray; separate experiments averaging multiple cells, selecting only responding cells) traces of HEK293T cells transfected with vectors containing various human (h) *TAS2R* sequences plus Gα16/gust44 as described in the text. Cells were stimulated with 100 µM *Pseudomonas* quinolone signal (PQS). Cells transfected with Gα16/gust44 (*a*) were used as a control ; T2Rs used were T2R4 (*b*), T2R5 (*c*), T2R14 (*d*), T2R16 (*e*), T2R38 (PAV isoform; *f*), T2R39 (*g*), T2R40 (*h*), T2R41 (*i*), and T2R46 (*j*). Peak responses are summarized in *k*. Known bitter compounds activating the transfected receptors were used as a positive control (1,2). Quinine and phenylthiocarbamide (PTC) were used as controls for T2R4 and T2R38, respectively, in separate experiments as shown in Fig 2. Purinergic agonist ATP was used as a positive control in cells transfected with Gα16/gust44 only.
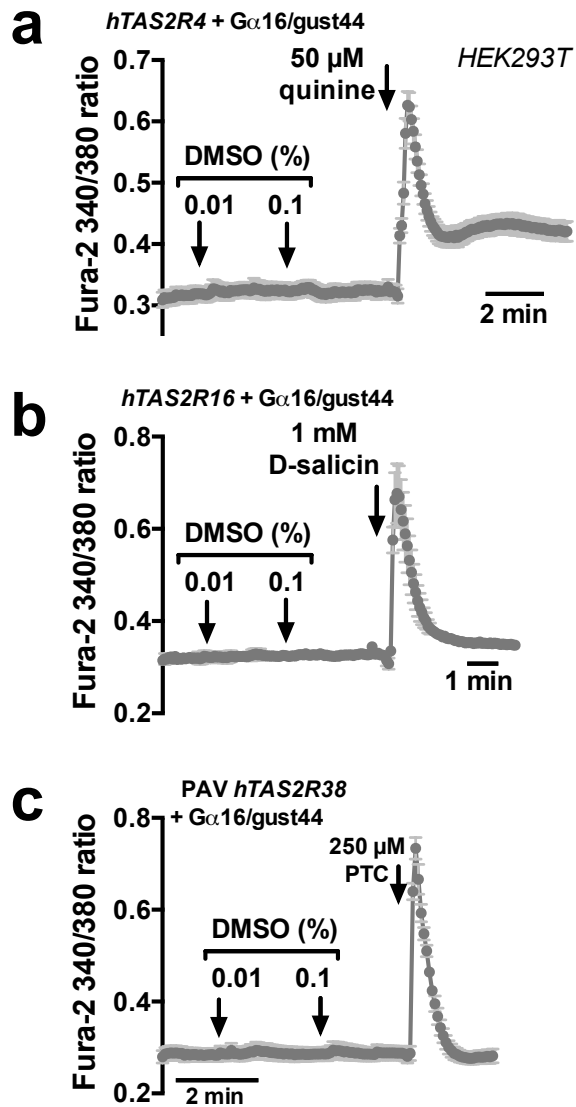
FIGURE S2. Vehicle control experiments for T2R stimulation. Final working solutions of PQS, HHQ, and DHQ contained a maximum 0.1% DMSO; We previously showed that T2R38 (3) and T2R14 (4) do not respond to 0.1% DMSO. We tested T2R4 (*a*), T2R16 (*b*), and again T2R38 (*c*) and found no response to 0.1% DMSO. Traces are mean ± SEM of 3-7 experiments each.
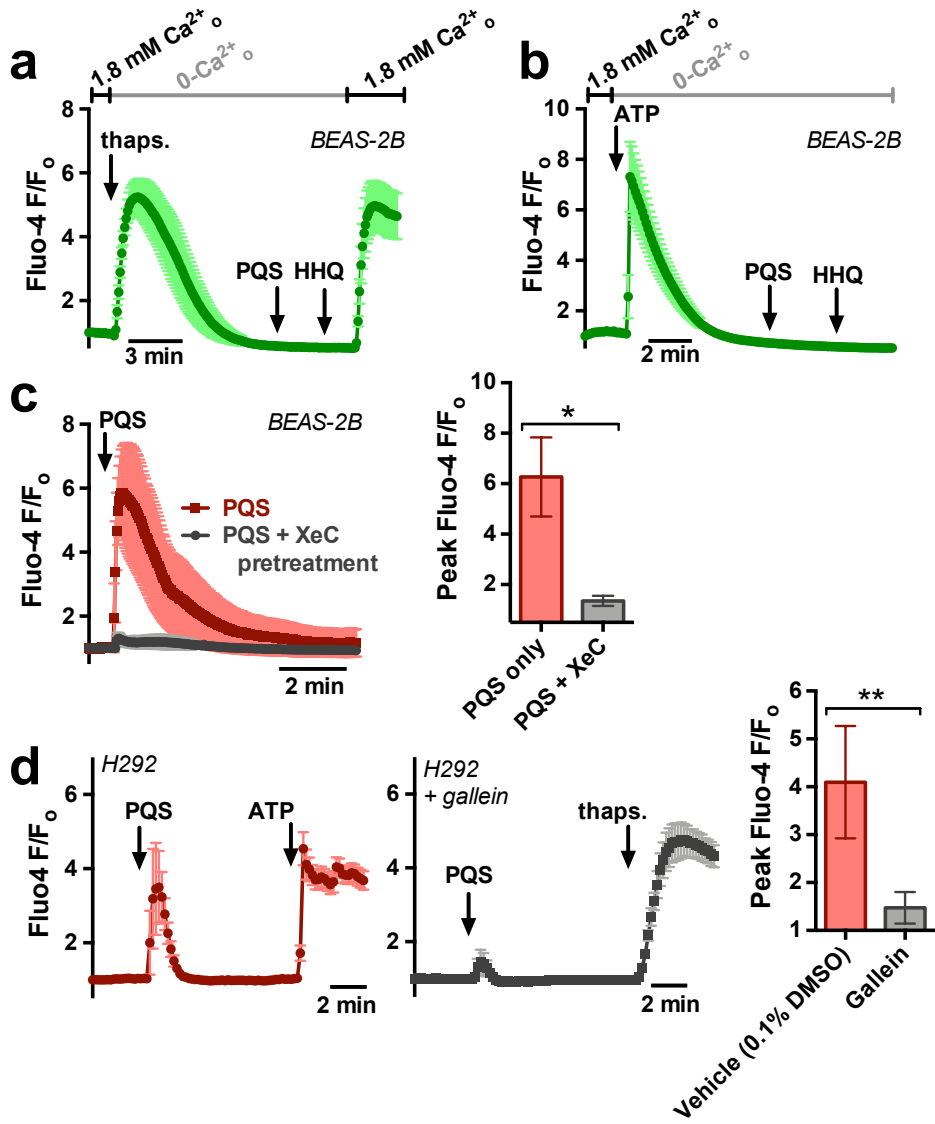
FIGURE S3. Quinolone-activated Ca^{2+} signals are dependent upon Ca^{2+} release from intracellular stores as well as G$\beta\gamma$ activation. *a-b*, Mean (±SEM) fluo-4 traces (n = 3-4 independent experiments each) showing lack of PQS or HHQ responses in BEAS-2B cells after Ca^{2+} store depletion by stimulation with the sarcoplasmic/endoplasmic reticulum Ca^{2+} ATPase SERCA pump inhibitor thapsigargin ((5); 5 µg/ml) or purinergic agonist ATP (100 µM) stimulation in 0-Ca^{2+} solution (2 mM EGTA). *c,* Mean (±SEM) fluo-4 traces (left) and peak response (right) to 100 µM PQS in BEAS-2B cells after pretreatment with IP$_3$ receptor inhibitor xestospongin C (XeC (6,7); 50 µM for 45 min). Significance determined by Student's t test; * p <0.05. *d*, H292 cells were loaded with fluo-4 and pretreated with the non-specific G$\beta\gamma$ inhibitor gallein (20 µM. 45 min; gray trace), a non-specific inhibitor of G$\beta\gamma$ function (8), or vehicle (0.1% DMSO; red trace) and stimulated with 100 µM PQS. Response was significantly inhibited in the presence of gallein (n = 6-9 experiments per condition). Significance of peak fluo-4 response determined by Student's *t* test; ** p <0.01.
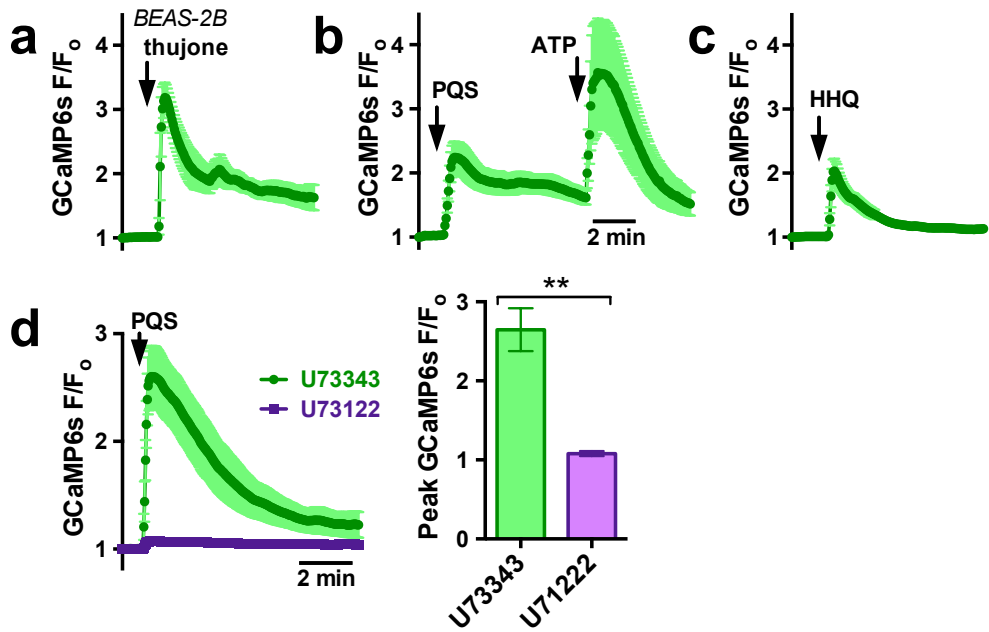
FIGURE S4. PQS and HHQ activate phospholipase C (PLC)-dependent Ca^{2+} responses in GCaMP6s-transfected BEAS-2B cells. Cells were transfected with GCaMP6s (9) and imaged as described in the text. ***a-c,*** Mean traces of GCaMP6s fluorescence with PQS (100 µM; *a*), HHQ (100 µM; *b*), and thujone (3 mM; *c*). ***d,*** Pretreatment (30 min; 10 µM) with PLC inhibitor U73122 (but not inactive U73343) blocked PQS-induced Ca^{2+} responses. All traces are mean ± SEM of 5-9 independent experiments. Significance in *d* determined by Student's *t* test; ** *p* <0.01.
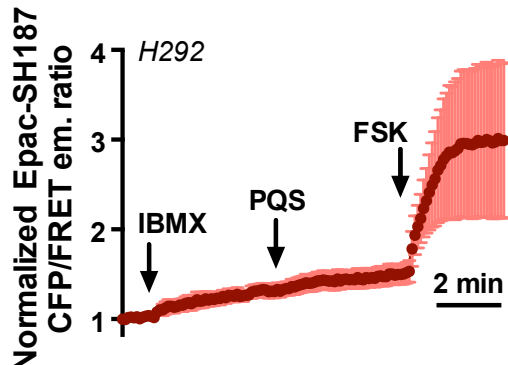
FIGURE S5. PQS (100 µM) did not reduce cAMP levels in the presence of IBMX (100 µM) in H292 cells transfected with EPAC-S[H187]; trace is mean ± SEM of 6 independent experiments.
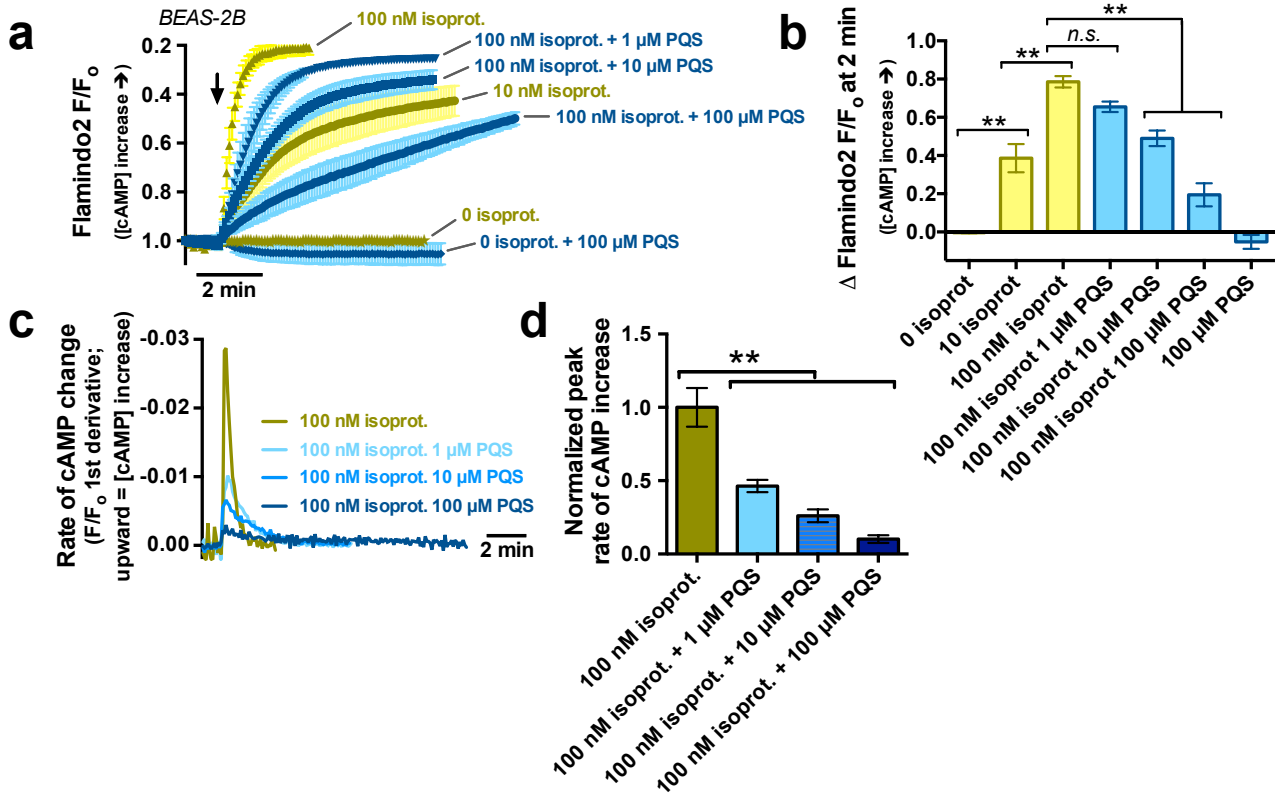
FIGURE S6. Dose-dependence of PQS effects on 100 nM isoproterenol-induced cAMP increases. *a*, Flamindo2 F/F_o traces (y-axis inverted; a decrease in F/F_o = an increase in $[cAMP]_i$) with lower levels (10-100 nM) isoproterenol (isoprot.) in the absence or presence of 1, 10, or 100 µM PQS in BEAS-2B cells. *b*, Bar graph showing change in Flamindo2 F/F_o after 2 min stimulation with indicated agonists. *c*, Graph of first derivative ($F/F_o \cdot sec^{-1}$) of indicated traces from *a* to illustrate kinetics of rate of cAMP increase. *d*, Bar graph (right) of mean ± SEM of the first derivatives of each individual experiment from *a* under the indicated conditions normalized to 100 nM isoproterenol alone to illustrate the magnitude of the impact of PQs on rate change. Significance determined by 1-way ANOVA with Bonferonni (*b*) or Dunnett (*d*) posttest; n = 4-5 independent experiments per condition. For bar graphs, * *p* <0.05 and ** *p* <0.01.
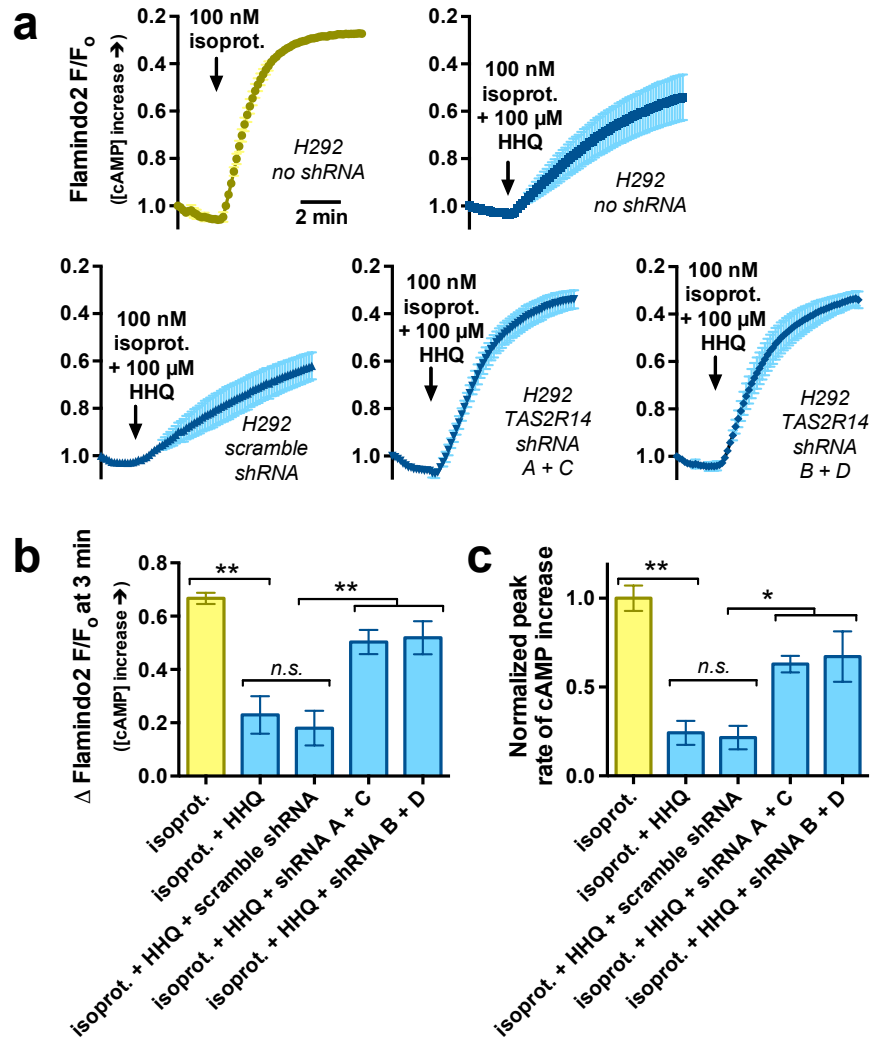
FIGURE S7. Inhibitory effects of 100 μM HHQ on 10 nM isoproterenol (isoprot.)-induced cAMP changes were blocked by T2R14 shRNAs. *a*, Mean ± SEM traces of Flamindo2 fluorescence (F/F_o) in H292 cells stimulated with 10 nM isoproterenol (isoprot.) ± 100 μM PQS under indicated transfection conditions (no shRNA, scramble shRNA, or T2R14-directed shRNAs A+C or B+D). *b-c*, Bar graphs of magnitude of Flamindo2 fluorescence changes after 3 min (*b*) and normalized rate of cAMP increase (*c*; as described in Supplemental Fig. 6). Significance determined by 1-way ANOVA with Bonferonni posttest; n = 3-5 independent experiments per condition. For bar graphs, * $p < 0.05$ and ** $p < 0.01$.
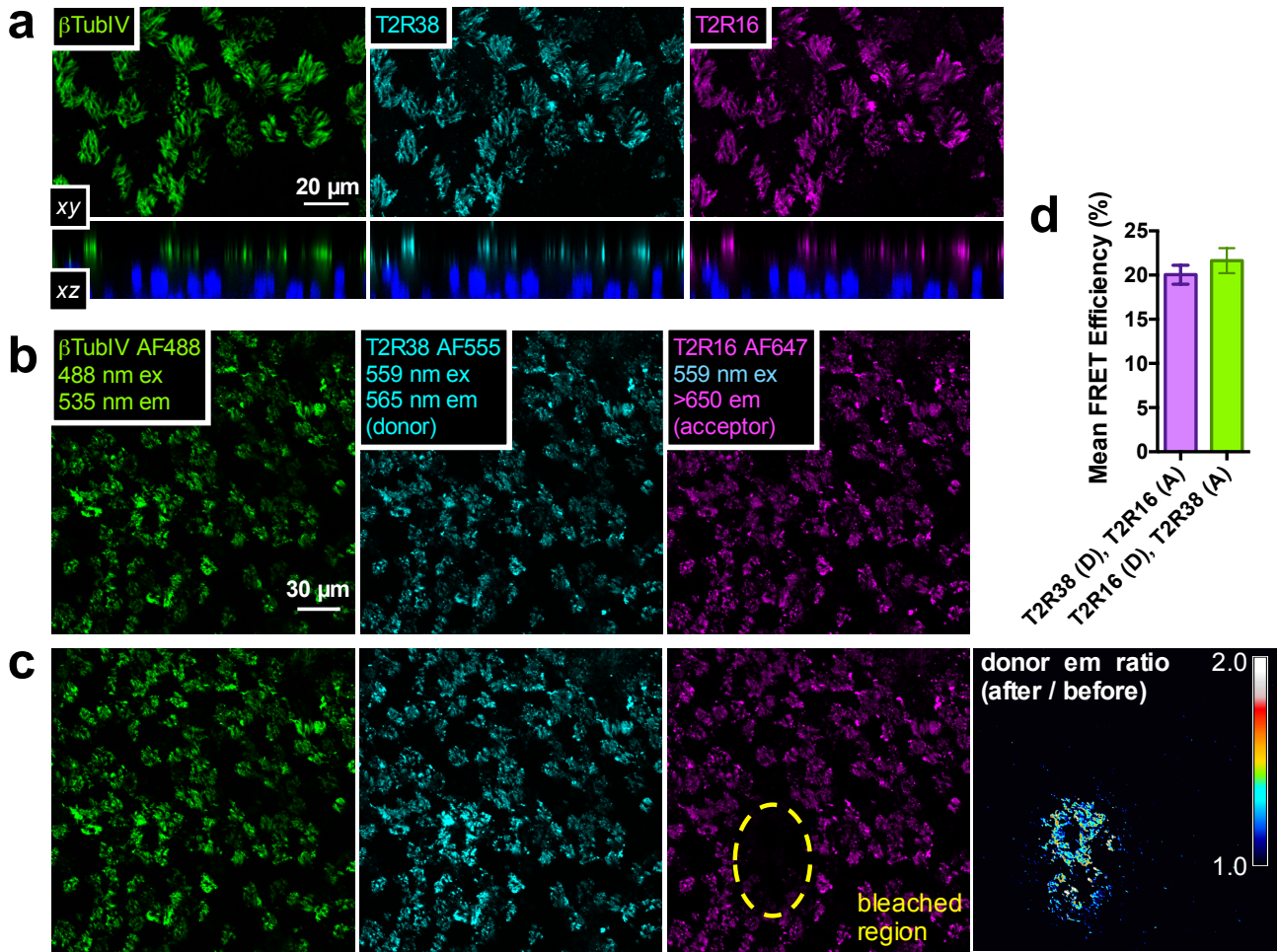
FIGURE S8. Co-localization of PQS-responsive T2R16 and T2R38 in primary sinonasal cell cilia. *a,* Immunofluorescence image (xy at top, xz orthogonal slice at bottom) of fixed primary sinonasal ALIs stained for cilia marker β-tubulin IV (βTubIV) as well as both T2R38 and T2R16 (primary antibodies directly labeled with AlexaFluor (AF) fluorophores). ***b-c,*** Immunofluorescence micrographs of AF488-labeled βTubIV with AF555 T2R38 and AF647 T2R16. T2R16 AF647 collected with AF555 T2R38 excitation as indicated. Images taken before (*b*) and after (*c*) photobleaching of area indicated by yellow oval with 647 nm laser (tornado bleaching function using SIM scanner and Olympus Fluoview software). Image on the far right is a ratio image showing the percent increase in T2R38 (donor) fluorescence with T2R16 (acceptor) bleaching. ***d,*** FRET efficiencies estimated from bleaching experiments as shown in *b*. Calculation of FRET efficiency, described in more detail in the text and in ref (4).

Compound	SMILES	Predicted as bitter?	Returned Probability for Activating Specific T2R Isoform									
			T2R1	T2R4	T2R10	T2R14	T2R16	T2R39	T2R40	T2R41	T2R43	T2R46
Quinine	COc1cc2c(ccnc2cc1)[C@H]([C@@H]1C[C@@H]2CCN1C[C@@H]2C=C)O	Yes	78%	74%	83%	74%	NP	74%	71%	76%	74%	74%
Chloroquine	Clc1cc2nccc(c2cc1)N[C@@H](C)CCCN(CC)CC	No	NP	NP	NP	NP	NP	NP	NP	NP	NP	NP
DHQ	c1ccc2[nH]c(=O)cc(O)c2c1	Yes	68%	55%	70%	75%	NP	53%	NP	70%	NP	NP
HHQ	CCCCCCCc1cc(=O)c2ccccc2[nH]1	No	NP	NP	NP	NP	NP	NP	NP	NP	NP	NP
PQS	CCCCCCCc1c(c(=O)c2ccccc2[nH]1)O	Yes	73%	64%	75%	74%	67%	75%	65%	75%	53%	NP

TABLE S1. Predictions of "bitterness" of *Pseudomonas* quinolones by BitterX (10). DHQ and PQS were predicted to activate several T2R receptors, while HHQ was not. Note that the well-documented T2R-activating compound chloroquine was also returned as "not bitter" by this software. Abbreviations used: DHQ, 2,4-dihydroxyquinolone; HHQ, 2-heptyl-4-quinolone; NP, not predicted by the software to activate indicate T2R; PQS, *Pseudomonas* quinolone signal (2-heptyl-3-hydroxy-4-quinolone). Database was accessed online at http://mdl.shsmu.edu.cn/BitterX/ on 6 July 2017 (for PQS, DHQ, HHQ), 20 July 2017 (for quinine), 17 August 2017 (for chloroquine). SMILES used for bitterness predictions (obtained from PubChem) are indicated.

Data values from bar graphs

Fig. 1*b*

	Gα16/gust4 4 only	*hTAS2R16*	*hTAS2R14*	*hTAS2R4*	*hTAS2R38*	*hTAS2R39*	*hTAS2R5*	*hTAS2R40*	*hTAS2R41*	*hTAS2R46*
Mean	0.01239	0.1336	0.03926	0.1994	0.08784	0.09801	0.01436	0.05358	0.01178	0.02489
SEM	0.002884	0.01825	0.006986	0.02326	0.01005	0.02319	0.003507	0.01767	0.003073	0.01248

Fig. 1*d*

	HHQ Gα16/gust 44 only	*HHQ hTAS2R4*	*HHQ hTAS2R14*	*HHQ hTAS2R16*	*HHQ hTAS2R38*	DHQ Gα16/gust44 only	*DHQ hTAS2R4*	*DHQ hTAS2R14*	*DHQ hTAS2R16*	*DHQ hTAS2R38*
Mean	0.008840	0.01955	0.06939	0.02590	0.03288	0.006857	0.01449	0.005382	0.007804	0.01798
SEM	0.001720	0.004063	0.02540	0.003890	0.005923	0.0007627	0.001789	0.001319	0.001906	0.003770

Fig. 2*c*

	Control PQS	GABA PQS	Control ATP	GABA ATP
Mean	0.3210	0.06301	0.6318	0.5987
SEM	0.03038	0.03975	0.05209	0.05582

Fig. 2*d*

	Control PQS	Proben PQS	Control salicin	Proben salicin	Control ATP	Proben ATP
Mean	0.195	0.02479	0.4248	0.04332	0.8003	0.8124
SEM	0.01546	0.01001	0.03857	0.01471	0.02263	0.02307

Fig. 2*e*

	PAV *hTAS2R38*	AVI *hTAS2R38*
Mean	0.1399	0.03031
SEM	0.01677	0.007165

Fig. 3*b*

	Vehicle	PQS	Quinine
Mean	0.00685	0.3095	0.6772
SEM	0.004858	0.04552	0.06401

Fig. 3*e*

	U73122	U73343
Mean	0.1101	0.6602
SEM	0.02325	0.08794

Fig. 4*e*

	HHQ				ATP				2FLI			
	no shRNA	*scramble*	*shRNA A+B*	*shRNA C + D*	no shRNA	*scramble*	*shRNA A+B*	*shRNA C + D*	no shRNA	*scramble*	*shRNA A+B*	*shRNA C + D*
Mean	1.564	1.705	0.3362	0.3952	2.409	2.714	1.995	2.110	2.622	2.623	2.586	2.349
SEM	0.1967	0.1206	0.1292	0.1382	0.3196	0.3217	0.3591	0.2277	0.2066	0.2162	0.3341	0.1225

Fig. 5*a*

	PQS	Quinine	Vehicle
Mean	-0.0575	-0.07009	-0.01151
SEM	0.009659	0.01467	0.008663

Fig. 5*b*

	Iso only	Iso + PQS
Mean	0.9256	0.4925
SEM	0.08996	0.1212

Fig. 5*c*

	Vehicle	PQS
Mean	-0.01867	-0.1098
SEM	0.01207	0.009009

Fig. 5*d*

	HHQ	DHQ
Mean	-0.08814	0.01999
SEM	0.01320	0.02021

Fig. 6*b*

	Vehicle + PQS	PTX + PQS	Vehicle + HHQ	PTX + HHQ
Mean	-0.1329	0.03787	-0.1048	-0.01328
SEM	0.04189	0.02107	0.01312	0.004556

Fig. *6c*

	EPAC-S^{H187} only	EPAC-S^{H187} + Wt gust	EPAC-S^{H187} + Gα16/gust44
Mean	-0.06089	-0.06955	0.01335
SEM	0.0079	0.01592	0.009244

Fig. 7*a*

	Control	+H89	Forskolin	Forskolin + H89
Mean	1.000	0.8511	1.413	0.9438
SEM	0.03509	0.03593	0.03033	0.01468

Fig. 7*b*

	Vehicle	PQS
Mean	0.01175	-0.05692
SEM	0.002470	0.01381

Fig. 8*d*

	Quinine	PQS	Vehicle (0.1% DMSO)	PQS + U73343	PQS + U73122
Mean	135.5	127.6	95.66	137	94.83
SEM	3.443	6.349	3.072	4.964	1.81

Fig. 9*a*

	0 PQS fsk	1 PQS fsk	10 PQS fsk	100 PQS fsk	0 PQS iso	1 PQS iso	10 PQS iso	100 PQS iso	0.1% DMSO fsk	0.1% DMSO iso
Mean	100	106.3	83.33	58	100	95.2	60.63	43.25	102.2	99.33
SEM	5.153	5.164	6.791	8.622	6.336	8.835	7.44	7.876	10.03	5.004

Fig. 9*b*

	0 PQS fsk + PTX	100 PQS fsk + PTX	0 PQS iso + PTX	100 PQS iso + PTX	0 PQS fsk	100 PQS fk	0 PQS iso	100 PQS iso
Mean	100	107	100	94	100	38	100	46
SEM	6	7	6	6	7	10	3	8

Fig. 10*b*

	PQS	PQS + D-NAME	PQS + L-NAME	PQS + DHQ + HHQ	PQS + DHQ + HHQ + L-NAME	Quinine	Quinine + L-NAME
Mean	231.2	210.3	14.99	395.2	14.60	344.4	7.438
SEM	20.95	16.75	4.044	36.91	6.027	44.00	2.647

Fig. 10*c*

	PAV Control	PAV Quinine	PAV PTC	PAV PQS	AVI Control	AVI Quinine	AVI PTC	AVI PQS	PAV FFA	AVI FFA
Mean	1.225	13.50	8.550	7.667	1.217	12.08	0.9083	5.250	7.083	8.833
SEM	0.4381	0.8944	0.5091	0.5110	0.3005	0.5833	0.2979	0.7159	0.8207	1.078

Fig. 10*d*

	PQS	PQS + probenecid + GABA
Mean	4.120	1.100
SEM	0.4510	0.2530

Supp Fig 1*k*

	Gα16/gust44 only	*hTAS2R16*	*hTAS2R14*	*hTAS2R4*	*hTAS2R38*	*hTAS2R39*	*hTAS2R5*	*hTAS2R40*	*hTAS2R41*	*hTAS2R46*
Mean	0.0285	0.2672	0.1052	0.3989	0.1749	0.196	0.0479	0.1541	0.03619	0.06514
SEM	0.00521	0.0365	0.0167	0.04653	0.01701	0.04638	0.01563	0.01369	0.006782	0.02048

Supp Fig. 3*c*

	PQS only	PQS + XeC
Mean	6.267	1.353
SEM	1.567	0.2012

Supp Fig. 3*d*

	Vehicle	Gallein
Mean	4.095	1.473
SEM	1.174	0.3300

Supp Fig. 4*d*

	U73343	U73122
Mean	2.645	1.080
SEM	0.2715	0.03138

Supp Fig 6*b*

	0 isoprot.	*1 nM isoprot.*	*10 nM isoprot.*	*10 nM isoprot. + 1 µM PQS*	*10 nM isoprot. + 10 µM PQS*	*10 nM isoprot. + 100 µM PQS*	*100 µM PQS*
Mean	-0.003711	0.3863	0.7858	0.6549	0.4898	0.1946	-0.05205
SEM	0.002988	0.07400	0.03000	0.02703	0.04071	0.06004	0.03639

Supp Fig 6*c*

	10 nM isoprot	10 nM isoprot. + 1 µM PQS	10 nM isoprot. + 10 µM PQS	10 nM isoprot. + 100 µM PQS
Mean	1.000	0.4635	0.2611	0.1017
SEM	0.1316	0.04198	0.04374	0.02618

Supp Fig 7*b*

	isoprot	*isoprot + HHQ*	*isoprot + HHQ + scramble shRNA.*	*isoprot + HHQ + shRNA A+C.*	*isoprot + HHQ + shRNA B+D.*
Mean	0.67	0.23	0.18	0.50	0.52
SEM	0.021	0.070	0.065	0.045	0.062

Supp Fig 7*d*

	isoprot	*isoprot + HHQ*	*isoprot + HHQ + scramble shRNA.*	*isoprot + HHQ + shRNA A+C.*	*isoprot + HHQ + shRNA B+D.*
Mean	1.00	0.2424	0.2154	0.6291	0.6715
SEM	0.072	0.068	0.066	0.047	0.14

Supp Fig 8*d*

	T2R38 (D), T2R16 (A)	**T2R16 (D), T2R38 (A)**
Mean	20.05	21.64
SEM	1.07	1.424

REFERENCES FOR SUPPORTING INFORMATION

1.   Wiener, A., Shudler, M., Levit, A., and Niv, M. Y. (2012) BitterDB: a database of bitter compounds. *Nucleic Acids Res.* **40**, D413-419
2.   Meyerhof, W., Batram, C., Kuhn, C., Brockhoff, A., Chudoba, E., Bufe, B., Appendino, G., and Behrens, M. (2010) The molecular receptive ranges of human TAS2R bitter taste receptors. *Chem. Senses* **35**, 157-170
3.   Lee, R. J., Xiong, G., Kofonow, J. M., Chen, B., Lysenko, A., Jiang, P., Abraham, V., Doghramji, L., Adappa, N. D., Palmer, J. N., Kennedy, D. W., Beauchamp, G. K., Doulias, P.-T., Ischiropoulos, H., Kreindler, J. L., Reed, D. R., and Cohen, N. A. (2012) T2R38 taste receptor polymorphisms underlie susceptibility to upper respiratory infection. *J. Clin. Invest.* **122**, 4145-4159
4.   Hariri, B. M., McMahon, D. B., Chen, B., Freund, J. R., Mansfield, C. J., Doghramji, L. J., Adappa, N. D., Palmer, J. N., Kennedy, D. W., Reed, D. R., Jiang, P., and Lee, R. J. (2017) Flavones modulate respiratory epithelial innate immunity: anti-inflammatory effects and activation of the T2R14 receptor. *J. Biol. Chem.* **292**, 8484-8497
5.   Thastrup, O., Cullen, P. J., Drobak, B. K., Hanley, M. R., and Dawson, A. P. (1990) Thapsigargin, a tumor promoter, discharges intracellular Ca2+ stores by specific inhibition of the endoplasmic reticulum Ca2(+)-ATPase. *Proc. Natl. Acad. Sci. U. S. A.* **87**, 2466-2470
6.   Miyamoto, S., Izumi, M., Hori, M., Kobayashi, M., Ozaki, H., and Karaki, H. (2000) Xestospongin C, a selective and membrane-permeable inhibitor of IP(3) receptor, attenuates the positive inotropic effect of alpha-adrenergic stimulation in guinea-pig papillary muscle. *Br. J. Pharmacol.* **130**, 650-654
7.   De Smet, P., Parys, J. B., Callewaert, G., Weidema, A. F., Hill, E., De Smedt, H., Erneux, C., Sorrentino, V., and Missiaen, L. (1999) Xestospongin C is an equally potent inhibitor of the inositol 1,4,5-trisphosphate receptor and the endoplasmic-reticulum Ca(2+) pumps. *Cell Calcium* **26**, 9-13
8.   Lehmann, D. M., Seneviratne, A. M., and Smrcka, A. V. (2008) Small molecule disruption of G protein beta gamma subunit signaling inhibits neutrophil chemotaxis and inflammation. *Mol. Pharmacol.* **73**, 410-418
9.   Chen, T. W., Wardill, T. J., Sun, Y., Pulver, S. R., Renninger, S. L., Baohan, A., Schreiter, E. R., Kerr, R. A., Orger, M. B., Jayaraman, V., Looger, L. L., Svoboda, K., and Kim, D. S. (2013) Ultrasensitive fluorescent proteins for imaging neuronal activity. *Nature* **499**, 295-300
10.   Huang, W., Shen, Q., Su, X., Ji, M., Liu, X., Chen, Y., Lu, S., Zhuang, H., and Zhang, J. (2016) BitterX: a tool for understanding bitter taste in humans. *Sci. Rep.* **6**, 23450